

THS



कार सम्बद्ध

THEORY OF THE MAGNETIC RESONANCE SPECTRA OF WATER-OF-HYDRATION AND METHYL PROTONS

Ву

Deborah May Roudebush

A THESIS

Submitted to
Michigan State University
in partial fulfillment of the requirements
for the degree of

MASTER OF SCIENCE

Department of Physics

13517

ABSTRACT

THEORY OF THE MAGNETIC RESONANCE SPECTRA OF WATER-OF-HYDRATION AND METHYL PROTONS

By

Deborah May Roudebush

The system of two quantum mechanical dipoles in different local magnetic fields is solved completely for the case of protons. Eigenvalues, transition energies, intensities, and spectra are given. The secular equation for three quantum mechanic dipoles in an equilateral triangular configuration in different local magnetic fields is found for protons. The symmetrical canting case, a special case for the three proton configuration, is treated with the eigenvalues found numerically at a number of geometric configurations.

ACKNOWLEDGMENTS

I wish to acknowledge Dr. Robert Spence for suggesting the problem and assisting with the experimentation. My deepest appreciation goes to Dr. Paul Parker for seeing me through to the end. I also wish to thank David Larch for his support and patience and Delores Sullivan for her skillful typing.

TABLE OF CONTENTS

Chapter		Page
I	INTRODUCTION	1
II	THE INTERACTION OF TWO QUANTUM MECHANICAL DIPOLES LOCATED IN DIFFERENT LOCAL MAGNETIC FIELDS	6
III	THE INTERACTION OF THREE QUANTUM MECHANICAL DIPOLES IN AN EQUILATERAL TRIANGULAR CONFIGURATION IN DIFFERENT LOCAL MAGNETIC FIELDS	26
IV	THE SYMMETRICAL CANTING CASE	41

LIST OF TABLES

Table		Page
1	Definitions of direction cosines, $\gamma,$ in the three-dipole triangular configuration	29
2	Definitions of scalar products, $\alpha\text{,}$ between coordinate systems in the three-dipole triangular configuration	29
3	The eigenvalues of the upper 3 x 3 submatrix as a function of θ in units of $C=(g_\beta)^2R^{-3}$	46

LIST OF FIGURES

Figure		Page
1.1	The 4.297 MHz resonance line.	3
2.1	Two protons separated by distance R and located in magnetic field \hat{H}_a and \hat{H}_b respectively. The fields are not necessarily coplanar.	10
2.2	Energy level diagram for the two dipole configuration in the general case.	10
2.3	Spectrum for the two dipole configuration in the general case.	12
2.4	Geometric configuration for two dipole case.	12
2.5	Energy level diagram for the two dipole configuration in limiting case A.	15
2.6	Spectrum for the two dipole configuration in limiting case A.	15
2.7	Energy level diagram for the two dipole configuration in limiting case B.	17
2.8	Spectrum for the two dipole configuration in limiting case B.	17
2.9	Energy level diagram and spectrum for the two dipole configuration in equal field case.	19
2.10	Plot of $\nu(\theta_{a},\theta_{b})$ where $\phi_{ab}\text{=}0$ for the two proton general case.	21
2.11	Plot of $\nu(\theta_{a},\theta_{b})$ where $\phi_{ab}\text{=}20^{\circ}$ for the two proton general case.	23
2.12	Plot of $v(\theta_a,\theta_b)$ where ϕ_{ab} =45° for the two proton general case.	25

Figure		Page
3.1	The equilateral triangular geometric configuration.	27
3.2	The Hamiltonian matrix for the three proton general case.	31
3.3	Geometric configuration with \vec{N} perpendicular to and directed out of the page. All vectors are coplanar.	36
3.4	Geometric configuration with \vec{a}_1 perpendicular to and directed out of the page. All vectors are coplanar.	37
3.5	Geometric configuration with $\stackrel{\rightarrow}{p}_{ab}$ perpendicular to and directed into the page. All vectors are coplanar.	37
4.1	The symmetrical canting case as seen in the plane containing pab and H at the proton a site.	42
4.2	The eigenvalues of the symmetrical canting case as a function of $\boldsymbol{\theta}.$	47
4.3	The geometric configuration for $\theta\!=\!\phi\!=\!90^\circ$. In this case $a_3\!=\!b_3\!=\!c_3$ and directed out of the page.	49
4.4	The geometric configuration for $\theta=150^{\circ}$, $\phi=180^{\circ}$. In this case $\hat{a}_1=\hat{b}_1=\hat{c}_1$ and directed out of the page.	49

CHAPTER I

INTRODUCTION

In their study of the antiferromagnetic crystal $CoCl_3((CH_3)_3NH)\cdot 2H_2O$, Spence and Botterman observed nuclear magnetic resonances (NMR) for the various protons in the crystal. The 17.64 MHz, the 16.80 MHz, and the 8.454 MHz proton resonances appear to have no splitting. The 5.955 MHz, the 3.359 MHz, and the 1.95 MHz proton resonance lines show dipole-like splitting. The line of particular interest, the 4.297 MHz proton resonance line, shows no typical dipole splitting. Instead it is made up of seven evenly spaced lines of varying intensity as shown in Figure 1.1. These resonances were all observed at approximately 2.4°K. The 4.297 MHz lines are field independent over a range from 125 G to 450 G.

In an effort to explain these lines, the general case of the dipole-dipole interaction is investigated since this corresponds to the physical situation of the protons of water of hydration units. The present study resulted in a complete solution for this geometry which can yield a maximum of only four lines. The Hamiltonian, secular equation, eigenvalues, eigenfunctions, and intensities are treated in detail. Also included are several limiting cases, including the "case of equal local magnetic fields" treated by Pake. ²

Figure 1.1. The 4.297 MHz resonance line.

3

_					1	1 .						<u> </u>	Τ-:		L	1	1
		;	1		-	+			†			<u> </u>	1	\$			1
				<u> </u>	 						-			₩			
									I		F = i = .	I	F	4			
					<u> </u>			L				L		<u>۔</u> ۔	!	L	
							, <u> </u>		†	· -			-	Y	1		
				0								<u> </u>		Λ	1.		
:			•	24.40 04.40	-			<u> </u>				<u> </u>		# \	1		
			. •			ļ · . ·			:					† 1 -	-		1
			1	4										T			
				Λ		1								£ - 1 -	1. = :		-
					-				-				-		1 -		-
E - :				- T		-						E		1	F-11-1		-
			1	1				_									
	-		- 1	1 1					<u> </u>						ļ		
-	<u> </u>		1	1									-			<u> </u>	
<u> </u>	-] - [-	 - 													
				1											!		
														F			
													-	1			-
			- 1											Ţ <u> </u>			
													H	1 :			
			1	t : : :	<u> </u>							_=:::::		+		: -:··:	
			1									===		+			
			H	L	1 -									<u> </u>	I		
			-		1							_		+	!		
			-		1										1 = :		:
			-										1				
			# . :		11								- ::	ļ ·			
					#=	-5								+			
			1		1	0	•	4	100				- 1	1	H		
								7	~					1	1		
					 	77		47	יַטַ יי	-	 ;				1		
		-				A		KV.	74.298	- V) *			1	II		
						F	.	4			ť						
				-	‡ ‡	1	1	~ :	, Y					†			
					1	1			A		1			-			-
	-				1	I		F	I	1			1	Ī —	\mathbf{H}^{-}		
		1			1	/				+				 			
		1		<u> </u>	- 1	T			<u> </u>	+			1 -	‡ - <u></u>			,
		1			V					Y			H	 			
		1	ļ <u></u> -	<u> </u>							1		1	<u> </u>			
-36	-	<u> </u>	·	<u> </u>	<u> </u>				<u> </u>			L		<u> </u>	M	-	

FIGURE I.I

Since protons exist in the equilateral triangular configuration in methyl groups, this geometry can also offer results of physical significance. This thesis presents an appropriate secular equation, which due to its complexity could not be solved analytically for the general case. For an arbitrarily chosen magnetic field direction, the secular equation was found to reduce to the "equal-field-case" as treated by Andrew and Bersohn. 3

A physically significant special case is obtained when the magnetic fields at the three proton sites of the equilateral triangle are taken such that the threefold symmetry of the geometrical configuration is retained. One such case of "symmetrical canting" requires that the three magnetic fields at the proton sites have equal magnitudes, and that their respective directions intersect on the threefold symmetry axis of the proton triangle. Such a case could conceivably apply at the methyl sites due to internal magnetic fields arising at cobalt sites located on or near the above threefold symmetry axis.

In this thesis, the secular equation for symmetrical canting is developed. Since only one angle is required to specify a particular canting configuration, it was found possible to solve the secular equation numerically for the eigenvalues for a series of angles of canting. The special case in which the magnetic fields are perpendicular to the plane of the methyl group triangle is an equal-field-case and is shown to properly reduce to the results of Andrew and Bersohn.

The three-proton case results in eight energy levels, and hence, can give rise to a maximum number of 28 possible transitions. If the dipole-dipole interactions are weak compared to the field-dipole

interactions, a maximum of 15 possible transitions can result in the general case. Thus, the observed splitting of the 4.297 MHz transition could possibly be accounted for in the proposed manner, but a much more detailed analysis would be required to be certain. Such an analysis will most likely have to include a study of the respective transition probabilities as well.

CHAPTER II

THE INTERACTION OF TWO QUANTUM MECHANICAL DIPOLES LOCATED IN DIFFERENT LOCAL MAGNETIC FIELDS

The Hamiltonian for two interacting dipoles in local magnetic fields \vec{H}_a and \vec{H}_b is given by the well-known expression 4

$$H = g\beta(H_{a}I_{a3} + H_{b}I_{b3}) + (g\beta)^{2}R^{-3} [\dot{T}_{a} \cdot \dot{T}_{b} - 3(\dot{T}_{a} \cdot \dot{p})(\dot{T}_{b} \cdot \dot{p})]$$
 (2.1)

Here \vec{p} is the unit vector between the two dipoles as shown in Figure 2.1. It is convenient to choose two Cartesian coordinate systems such that the local axis of quantization is along the local field at each dipole. These axes will be indicated as the respective 3-axis. The 2-axis will be in the plane determined by the 3-axis and \vec{p} . The right hand rule then determines the 1-axis. The unit vectors of each system will be designated by the letter of the nucleus at the site; i.e. \vec{a}_i at proton a, and \vec{b}_i at proton b.

On defining the scalar products,

$$\vec{I}_{a} \cdot \vec{p} = \sum_{i} \gamma_{ai} I_{ai} \qquad \vec{I}_{b} \cdot \vec{p} = \sum_{j} \gamma_{bj} I_{bj}$$

$$\vec{I}_{a} \cdot \vec{I}_{b} = \sum_{i,j} \alpha_{ij} I_{ai} I_{bj}$$
(2.2)

where γ_{ai} is the direction cosine of \vec{p} in the \vec{a}_i direction, γ_{bi} is the direction cosine of \vec{p} in the \vec{b}_i direction and α_{ij} is the cosine of the angle between \vec{a}_i and \vec{b}_j , the Hamiltonian may be written as

$$H = g\beta(H_{a}I_{a3} + H_{b}I_{b3}) - C\sum_{i}\sum_{j} (3\gamma_{ai}\gamma_{bj} - \alpha_{ij})I_{ai}I_{bj}$$
 (2.3)

where

$$C \equiv (g\beta)^2 R^{-3} \tag{2.4}$$

With the further definition

$$D_{ij} = -\frac{1}{4}C(3\gamma_{ai}\gamma_{bj}-\alpha_{ij}) \qquad (2.5)$$

The Hamiltonian becomes

$$H = g\beta(H_{a}I_{a3} + H_{b}I_{b3}) + 4\sum_{i,j} D_{ij}I_{ai}I_{bj}$$
 (2.6)

If $I = \frac{1}{2}$, which is the case for protons, then in the basis indicated below, the block diagonal matrix of the Hamiltonian is found to be the following:

Basis:

where $D = -D_{33}$. One can immediately write down two eigenvalues, viz.,

$$E_{1} = \frac{1}{2}g\beta(H_{a} + H_{b}) - D$$

$$(2.8)$$

$$E_{4} = -\frac{1}{2}g\beta(H_{a} + H_{b}) - D$$

In order to obtain the remaining two eigenvalues, let

$$\Delta \equiv (D_{11} + D_{22}) + i(D_{12} - D_{21}) \tag{2.9}$$

which yields the secular equation

$$(E-D)^2 = \frac{1}{4}(g\beta\Delta H)^2 + |\Delta|^2$$
 (2.10)

where $\Delta H = H_a - H_b$, with roots

$$E_{2,3} = D \pm (\frac{1}{4}(g\beta\Delta H)^2 + |\Delta|^2)^{\frac{1}{2}}$$
 (2.11)

The general solution, therefore, is

$$E_{1} = g\beta H_{ave} - D$$

$$E_{2} = S + D$$

$$E_{3} = -S + D$$

$$E_{4} = -g\beta H_{ave} - D$$
(2.12)

where

$$S = ((\frac{1}{2}g\beta\Delta H)^2 + |\Delta|^2)^{\frac{1}{2}}$$
 (2.13)

and

$$H_{ave} = \frac{1}{2}(H_a + H_b)$$
 (2.14)

In the diagonalized basis, the corresponding normalized basis functions are found to be

$$\psi_{1} = (2S^{2} + g\beta\Delta HS)^{-\frac{1}{2}} [(-\frac{1}{2}g\beta\Delta H - S)(+-) - \Delta^{*}(-+)]$$

$$\psi_{2} = (2S^{2} - g\beta\Delta HS)^{-\frac{1}{2}} [(-\frac{1}{2}g\beta\Delta H + S)(+-) - \Delta^{*}(-+)]$$
(2.15)

The transition probabilities are proportional to $|\langle n|I_X|n'\rangle|^2$ where n and n' are the initial and final states between which magnetic dipole transitions are considered. In the two-dipole interaction, this calculation yields

$$\pm 2D+S$$
: $\frac{1}{4}[1 + \frac{(2S+g\beta\Delta H)Re\Delta}{2S^2+g\beta\Delta HS}]$
 $\pm 2D-S$: $\frac{1}{4}[1 + \frac{(2S-g\beta\Delta HS)Re\Delta}{2S^2-g\beta\Delta HS}]$ (2.16)

where the left column is the change in energy of transition from the unperturbed value and the right hand column is the corresponding normalized transition probability.

The energy levels are shown in Figure 2.2 with the transition energies as follows:

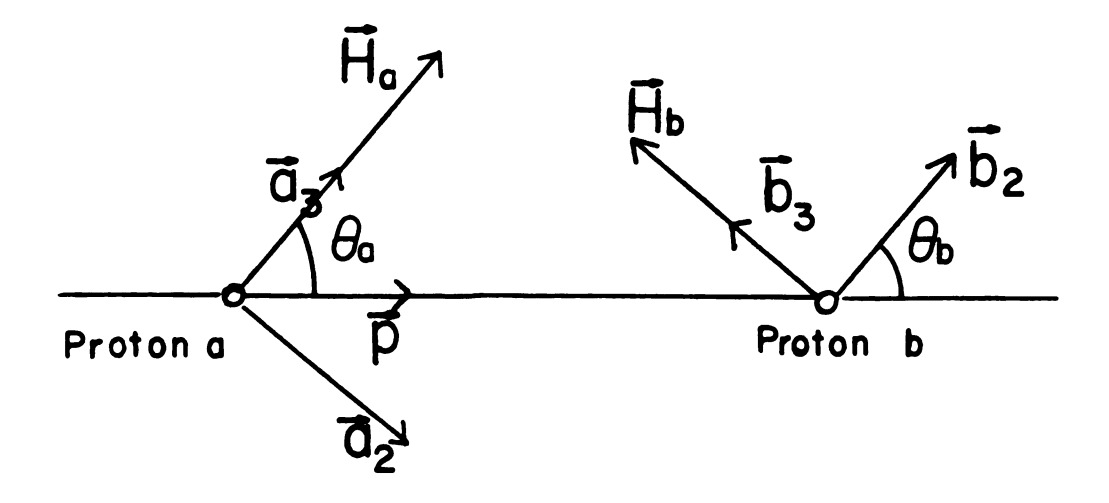


Figure 2.1. Two protons separated by distance R and located in magnetic field \hat{H}_a and \hat{H}_b respectively. The fields are not necessarily coplanar.

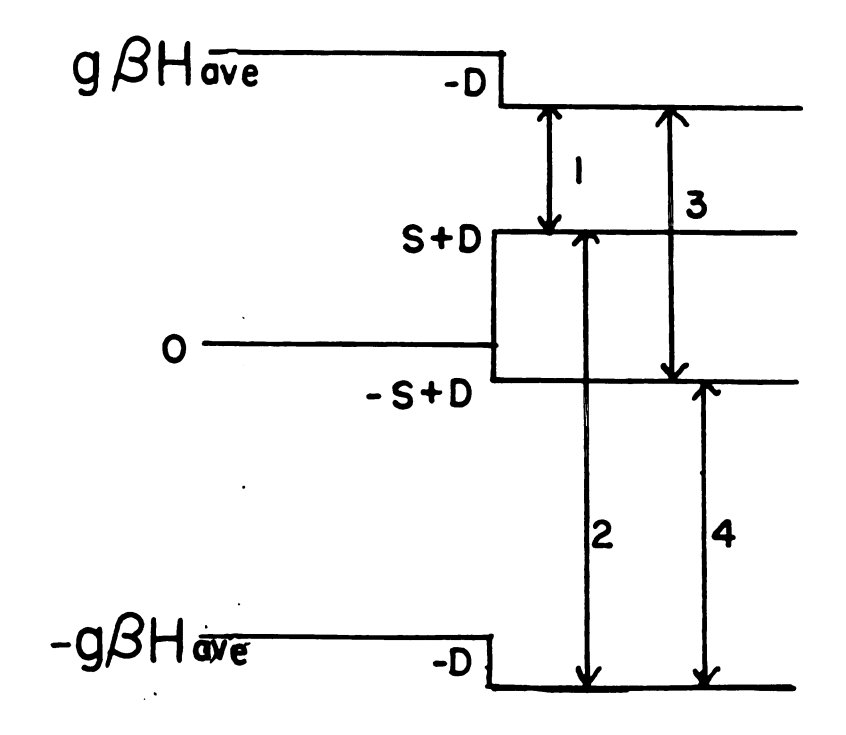


Figure 2.2. Energy level diagram for the two dipole configuration in the general case.

$$hv_1 = g\beta H_{ave} - 2D - S$$

$$hv_2 = g\beta H_{ave} + 2D + S$$

$$hv_3 = g\beta H_{ave} - 2D + S$$

$$hv_4 = g\beta H_{ave} + 2D - S$$

$$(2.17)$$

These energies yield the spectrum shown in Figure 2.3.

Referring to Figure 2.1 and Figure 2.4, the following relations may be determined:

$$\gamma_{a1} = 0 \qquad \gamma_{b1} = 0$$

$$\gamma_{a2} = \sin\theta_{a} \qquad \gamma_{b2} = \sin\theta_{b}$$

$$\gamma_{a3} = \cos\theta_{a} \qquad \gamma_{b3} = \cos\theta_{b}$$

$$\alpha_{11} = \vec{a}_{1} \cdot \vec{b}_{1} = \cos\phi_{ab}$$

$$\alpha_{22} = \vec{a}_{2} \cdot \vec{b}_{2} = \sin\theta_{a} \sin\theta_{b} + \cos\theta_{a} \cos\theta_{b} \cos\phi_{ab}$$

$$\alpha_{33} = \vec{a}_{3} \cdot \vec{b}_{3} = \cos\theta_{a} \cos\theta_{b} + \sin\theta_{a} \sin\theta_{b} \cos\phi_{ab} = \cos\theta_{ab}$$

$$\alpha_{12} = \vec{a}_{1} \cdot \vec{b}_{2} = \sin\phi_{ab} \cos\theta_{b}$$

$$\alpha_{21} = \vec{a}_{2} \cdot \vec{b}_{1} = -\sin\phi_{ab} \cos\theta_{a}$$
(2.18)

Inserting these results into Equation 2.4 and Equation 2.7, the geometrical relations for D and $\left|\Delta\right|^2$ become

$$D = \frac{1}{4}g^{2}\beta^{2}R^{-3}(3\cos\theta_{a}\cos\theta_{b}-\cos\theta_{ab})$$

$$|\Delta|^{2} = (\frac{1}{4}g^{2}\beta^{2}R^{-3})^{2} \{ (3\cos\theta_{a}\cos\theta_{b}-\cos\theta_{ab})^{2}$$

$$+ 4(1-\cos\theta_{ab}) -3(\cos\theta_{a}-\cos\theta_{b})^{2} \}$$
(2.19)

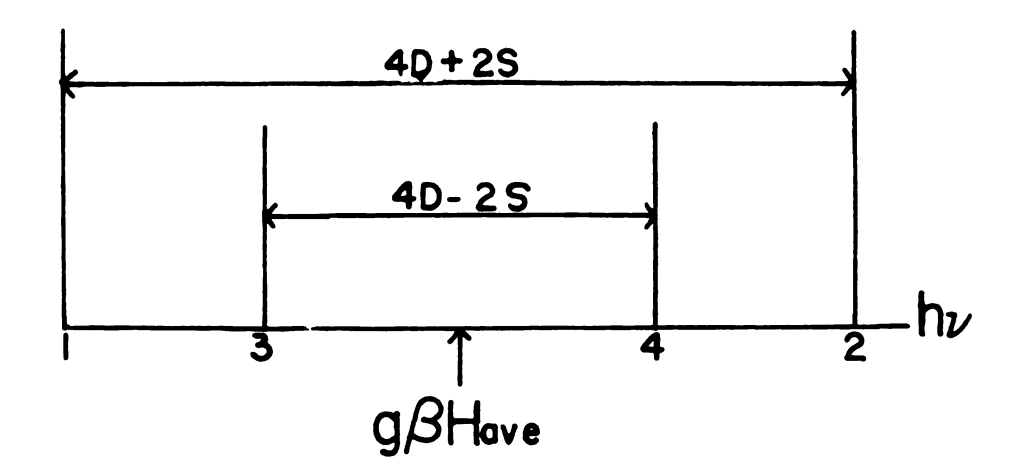
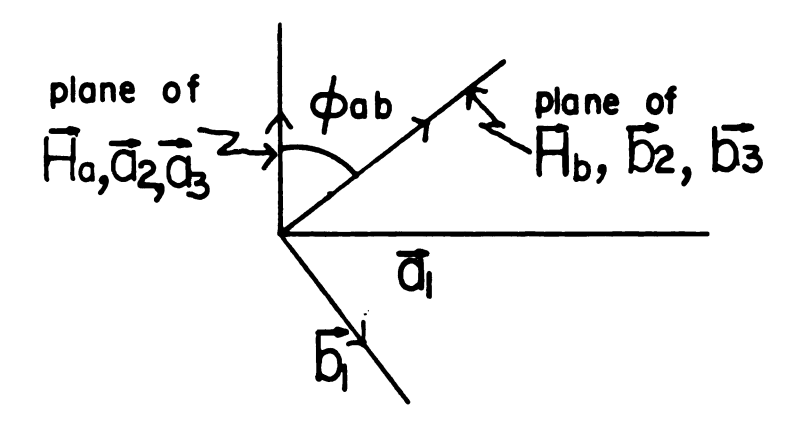


Figure 2.3. Spectrum for the two dipole configuration in the general case.



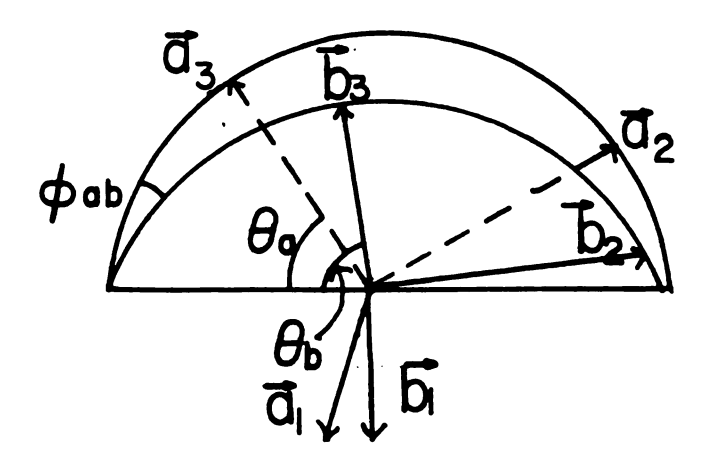


Figure 2.4. Geometric configuration for two dipole case.

These results agree with the results given by G.E.G. Hardeman⁵ in his dissertation and credited to J. D. Poll.

Limiting Cases

A. Consider the case where $|\Delta|^2 << (\frac{1}{2} g \beta \Delta H)^2$, i.e. $H_a >> H_b$ or $H_a << H_b$. Then

$$S \cong \frac{1}{2}g\beta\Delta H + |\Delta|^2(g\beta\Delta H)^{-1}$$
 (2.20)

yielding eigenvalues of

$$E_{1} = g\beta H_{ave} - D$$

$$E_{2} = \pm \frac{1}{2}g\beta\Delta H + D + \delta$$

$$E_{3} = \pm \frac{1}{2}g\beta\Delta H + D - \delta$$

$$E_{4} = -g\beta H_{ave} - D$$
(2.21)

where

$$\delta = |\Delta|^2 (g\beta\Delta H)^{-1} \tag{2.22}$$

and E₁ and E₄ are exact. The top sign of the double sign refers to $\vec{H}_a >> \vec{H}_b$ and the bottom sign refers to $\vec{H}_a << \vec{H}_b$.

The energy levels are as shown in Figure 2.5 with the transition energies as follows:

$$hv_{1} = g\beta H_{ave} - \frac{1}{2}g\beta\Delta H - 2D - \delta$$

$$hv_{2} = g\beta H_{ave} + \frac{1}{2}g\beta\Delta H + 2D + \delta$$

$$hv_{3} = g\beta H_{ave} + \frac{1}{2}g\beta\Delta H - 2D + \delta$$

$$hv_{4} = g\beta H_{ave} - \frac{1}{2}g\beta\Delta H + 2D - \delta$$

$$(2.23)$$

This yields the spectrum shown in Figure 2.6. For very large $|\Delta H|$, δ is negligible compared to $\frac{1}{2}g\beta\Delta H$.

B. Consider the case where $|\Delta|^2 >> (\frac{1}{2}g\beta\Delta H)^2$, i.e. $H_a \approx H_b$. Now

$$S = |\Delta| + \frac{1}{2} |\Delta|^{-1} (\frac{1}{2} g \beta \Delta H)^2$$
 (2.24)

yielding eigenvalues of

$$E_{1} = g\beta H_{ave} - D$$

$$E_{2} = D + |\Delta| + \varepsilon$$

$$E_{3} = D - |\Delta| - \varepsilon$$

$$E_{4} = -g\beta H_{ave} - D$$
(2.25)

where

$$\varepsilon = \frac{1}{2} |\Delta|^{-1} \left(\frac{1}{2} g \beta \Delta H\right)^2 \tag{2.26}$$

and \mathbf{E}_1 and \mathbf{E}_2 are exact. The energy level diagram is given as Figure 2.7.

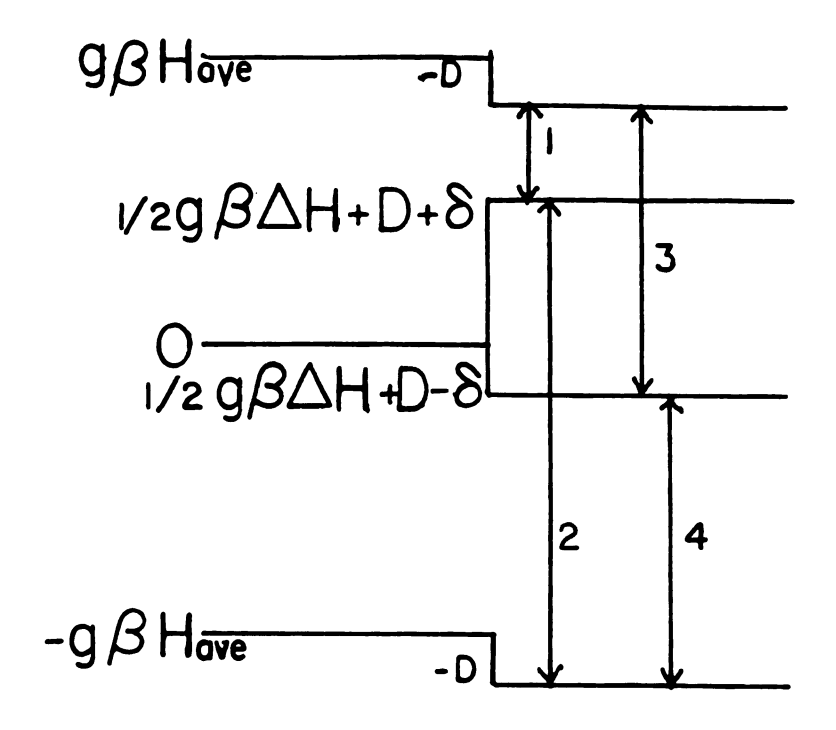


Figure 2.5. Energy level diagram for the two dipole configuration in limiting case A.

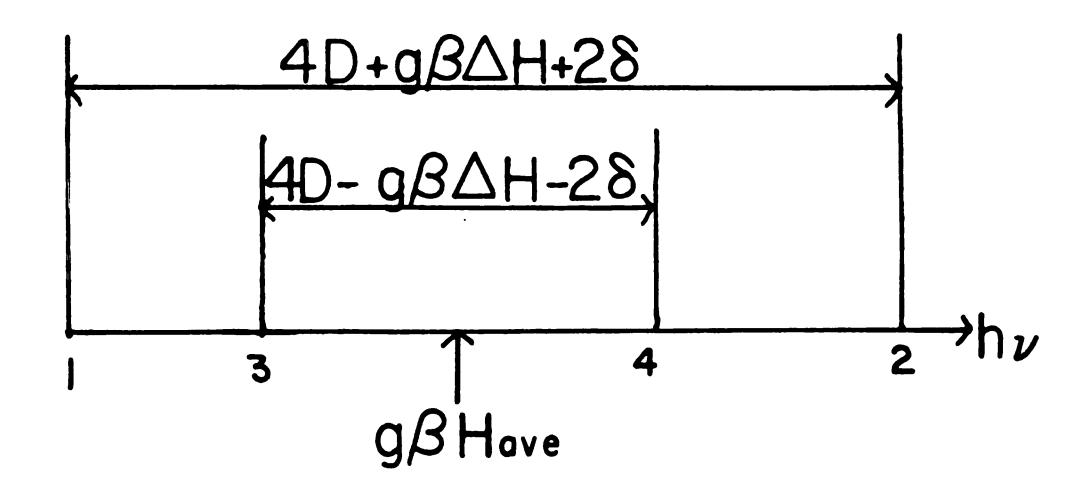


Figure 2.6. Spectrum for the two dipole configuration in limiting case A.

The transition energies are as follows

$$hv_{1} = g\beta H_{ave} - 2D - |\Delta| - \epsilon$$

$$hv_{2} = g\beta H_{ave} + 2D + |\Delta| + \epsilon$$

$$hv_{3} = g\beta H_{ave} - 2D + |\Delta| + \epsilon$$

$$hv_{4} = g\beta H_{ave} + 2D - |\Delta| - \epsilon$$

$$(2.27)$$

with the spectrum shown in Figure 2.8. If ΔH becomes very small, then ϵ goes to zero.

C. For the special case that the two magnetic fields are equal in direction and magnitude,

$$\vec{H}_a = \vec{H}_b, |\vec{H}_a| = |\vec{H}_b| = H, \alpha_{ij} = \vec{a}_i \cdot \vec{b}_j = \delta_{ij}$$
 (2.28)

Equation 2.5 reduces readily to the Hamiltonian which applies in this case, viz., the one given by Pake. 2 It follows that ϕ_{ab} =0, θ_a = θ_b = θ , and therefore D and $|\Delta|^2$ reduce to

$$D = \frac{1}{4}C (3\cos^2\theta - 1)$$

$$|\Delta|^2 = (D_{11} + D_{22})^2 = (\frac{1}{4}C)^2 (3\cos^2\theta - 1)^2$$

$$|\Delta| = D$$
(2.29)

The eigenvalues reduce to

$$E_1 = g\beta H - D$$
 $E_2 = 2D$
 $E_3 = 0$
 $E_4 = -g\beta H - D$

(2.30)

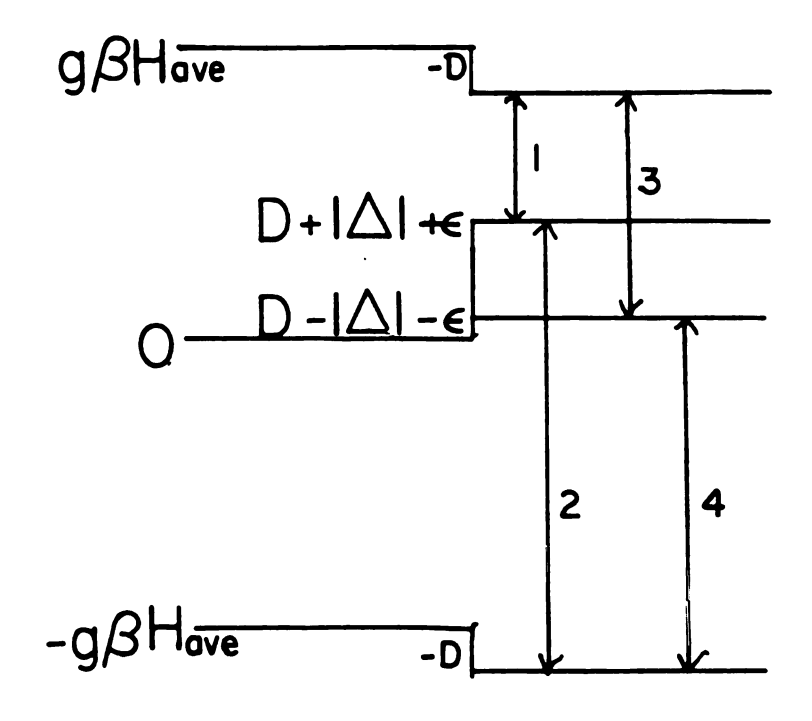


Figure 2.7. Energy level diagram for the two dipole configuration in limiting case B.

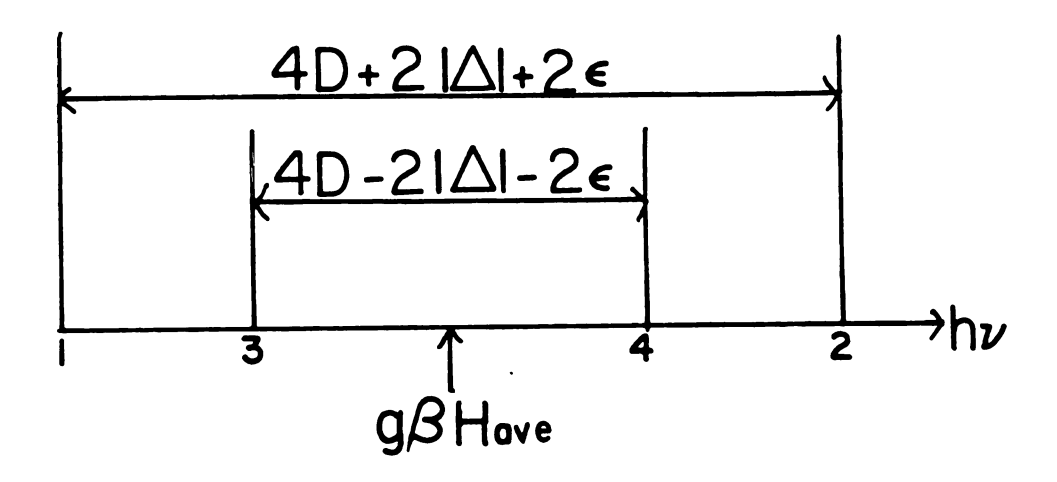


Figure 2.8. Spectrum for the two dipole configuration in limiting case B.

as in Pake, with transition energies

$$hv_1 = g\beta H - 3D$$

$$hv_2 = g\beta H + 3D$$

$$hv_3 = g\beta H - D$$

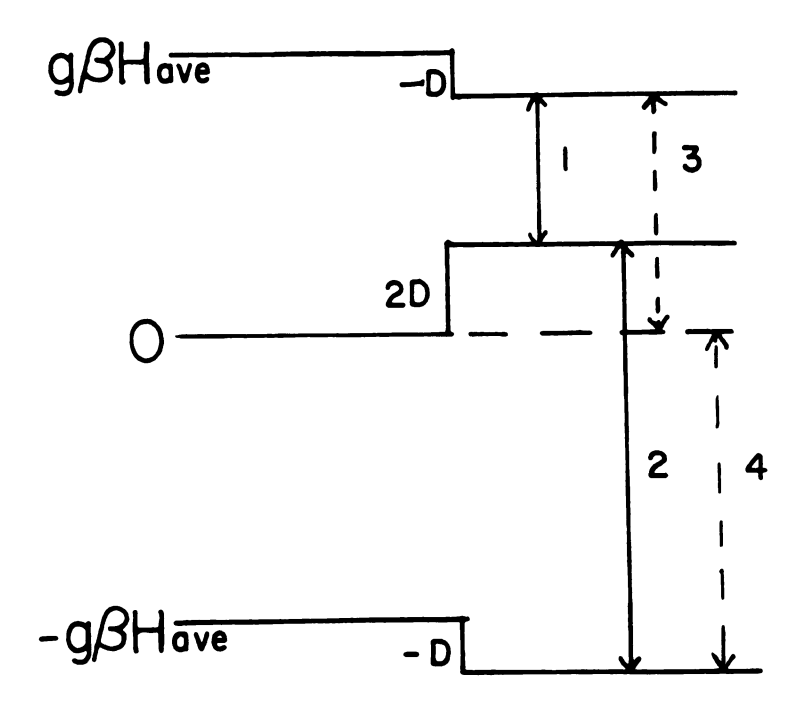
$$hv_4 = g\beta H + D$$
(2.31)

The transitions hv_3 and hv_4 are the forbidden singlet-triplet transition as shown in Figure 2.9. The intensities reduce to $\frac{1}{2}$, $\frac{1}{2}$, and 0 as required by the Pake solution.

For the general case, the frequencies were plotted using the Hewlett-Packard 9100B three dimensional perspective plot routine. The local magnetic field values and ϕ_{ab} were held constant throughout a given plot, while θ_a and θ_b were varied. Each plot has ν_2 in black and ν_3 in red and is centered about

$$h^{-1}(g\beta H_{ave} + [(\frac{1}{2}g\beta\Delta H)^2 - |\Delta|^2)]^{\frac{1}{2}})$$
 (2.32)

The field dependence of the frequencies is so small that these perturbations are not observable on the plots. The ϕ_{ab} dependence and therefore the θ_{ab} dependence is small, but can be seen by comparing closely Figure 2.10, Figure 2.11, and Figure 2.12.



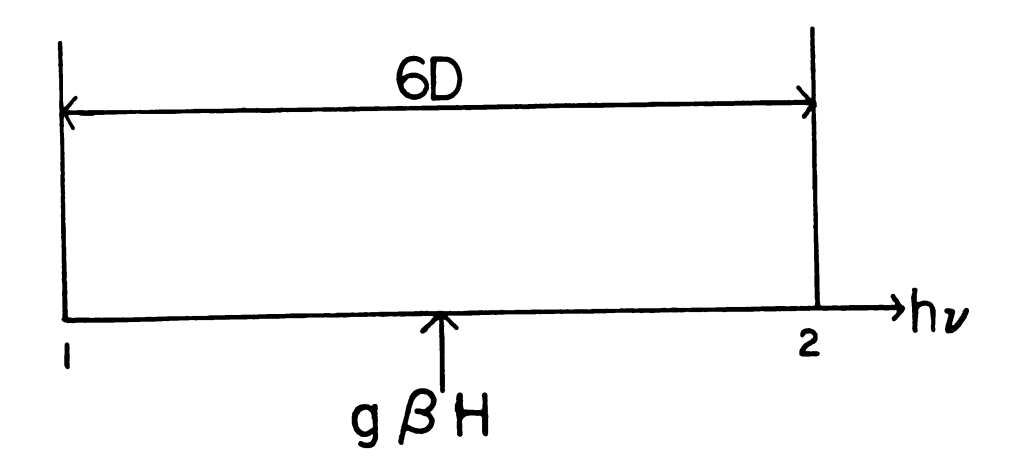


Figure 2.9. Energy level diagram and spectrum for the two dipole configuration in equal field case.

Figure 2.10. Plot of $\nu(\theta_a,\theta_b)$ where $\phi_{ab}\text{=}0$ for the two proton general case.

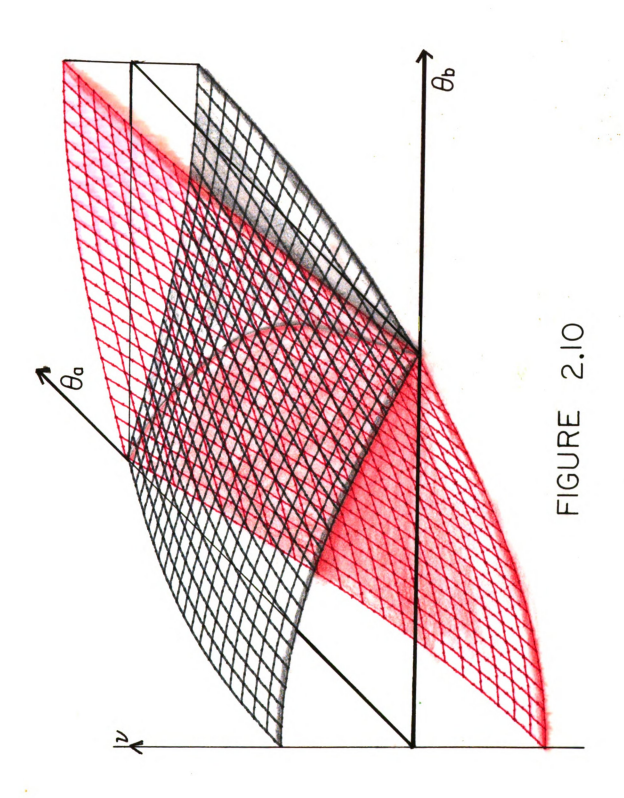


Figure 2.11. Plot of $\nu(\theta_a,\theta_b)$ where ϕ_{ab} =20° for the two proton general case.

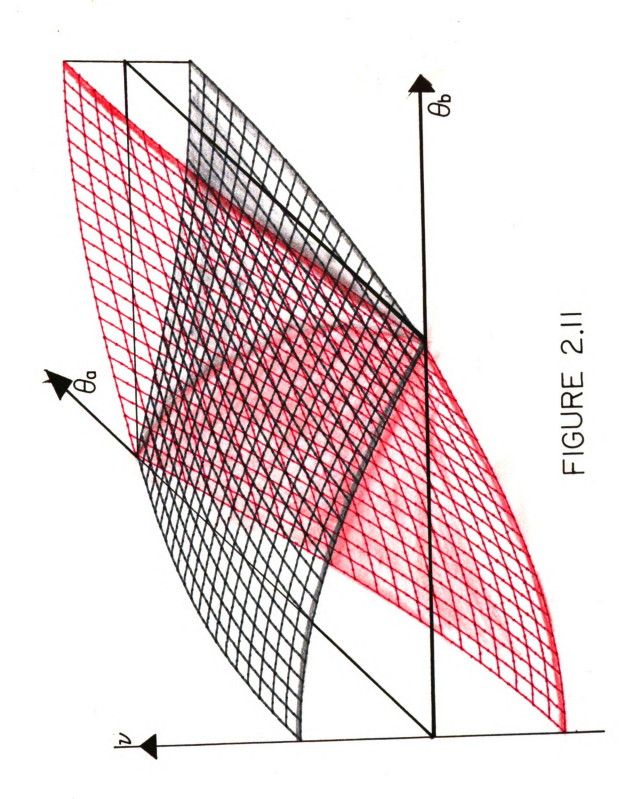
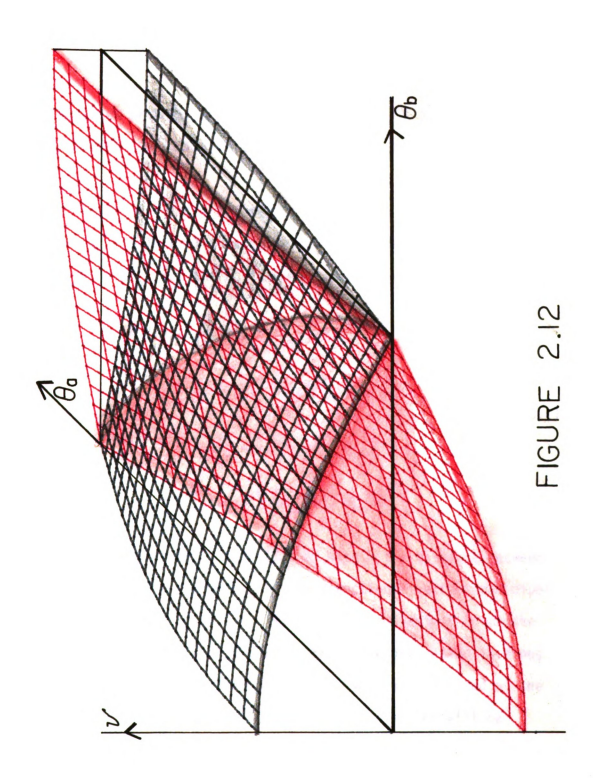


Figure 2.12. Plot of $\nu(\theta_a,\theta_b)$ where $\phi_{ab}\text{=}45^\circ$ for the two proton general case.



CHAPTER III

THE INTERACTION OF THREE QUANTUM MECHANICAL DIPOLES IN AN EQUILATERAL
TRIANGULAR CONFIGURATION IN DIFFERENT LOCAL MAGNETIC FIELDS

The Hamiltonian for the interaction of three quantum mechanical dipoles in an equilateral triangular configuration in different local magnetic fields \vec{H}_a , \vec{H}_b , and \vec{H}_c follows readily from (2.1) as

$$H = g\beta(\vec{H}_{a} \cdot \vec{T}_{a} + \vec{H}_{b} \cdot \vec{T}_{b} + \vec{H}_{c} \cdot \vec{T}_{c})$$

$$+ C[\vec{T}_{a} \cdot \vec{T}_{b} - 3(\vec{T}_{a} \cdot \vec{p}_{ab})(\vec{T}_{b} \cdot \vec{p}_{ab})]$$

$$+ C[\vec{T}_{b} \cdot \vec{T}_{c} - 3(\vec{T}_{b} \cdot \vec{p}_{bc})(\vec{T}_{c} \cdot \vec{p}_{bc})]$$

$$+ C[\vec{T}_{c} \cdot \vec{T}_{a} - 3(\vec{T}_{c} \cdot \vec{p}_{ca})(\vec{T}_{a} \cdot \vec{p}_{ca})]$$

$$(3.1)$$

where C is defined as in Chapter II, and with R the distance between any two dipoles. The vector \vec{p}_{ij} is the directional vector from dipole i to dipole j, as in Figure 3.1. Again, it is convenient to choose coordinate systems such that the local axis of quantization is along the field at each dipole. These axes will again be indicated as the 3-axis in each system. The unit vectors of each system will be designated by the letter of the nucleus at that site, i.e., \vec{a}_i at proton a, etc.

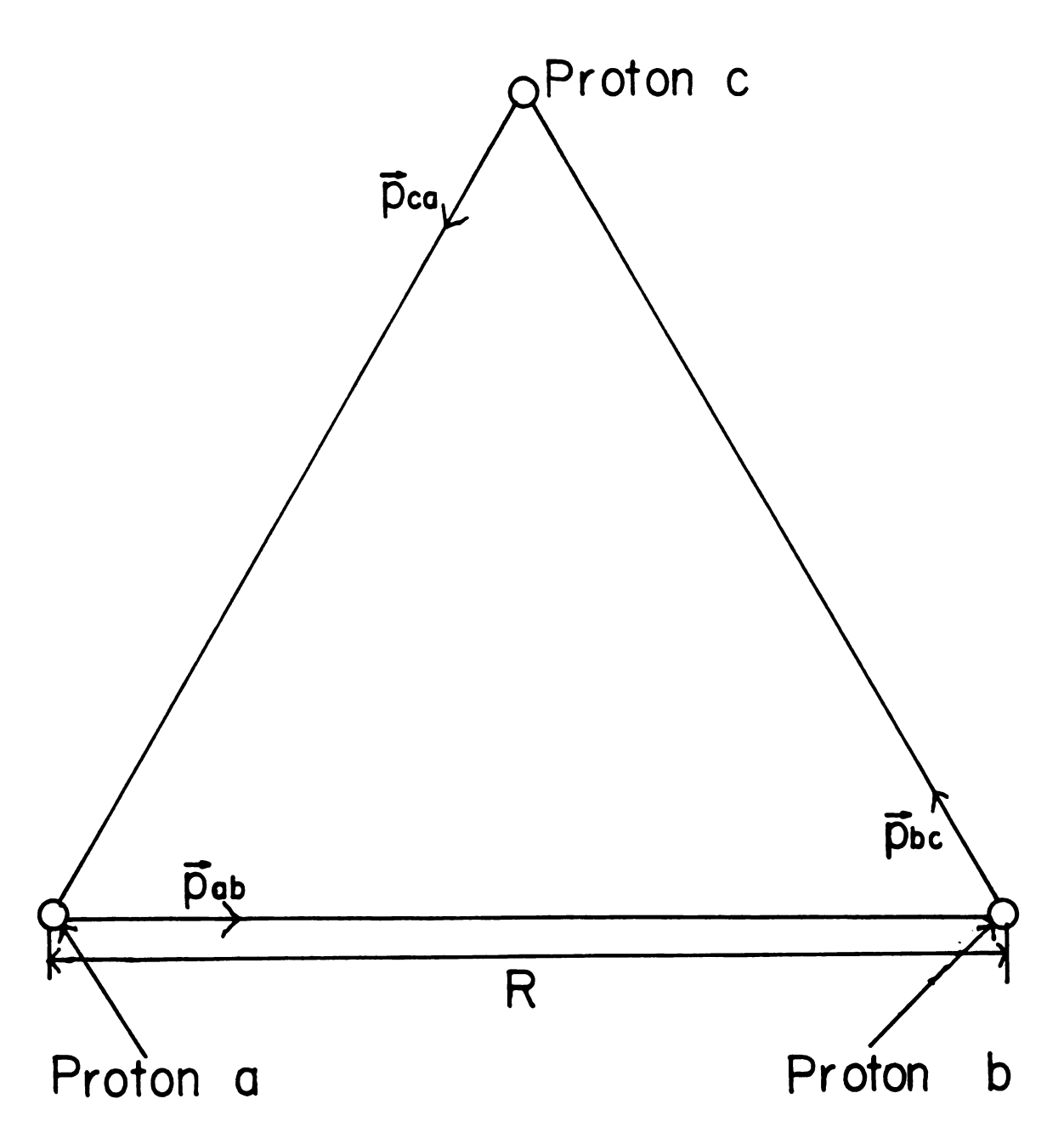


Figure 3.1. The equilateral triangular geometric configuration.

On defining the scalar products as in Table 1 and Table 2, the Hamiltonian, Equation 3.1, may be written

$$H = g\beta(H_{a}I_{a3}+H_{b}I_{b3}+H_{c}I_{c3})$$

$$-C\sum_{ij} (3\gamma_{ai}^{ab}\gamma_{bj}^{ab}-\alpha_{ij}^{ab})I_{ai}I_{bj}$$

$$-C\sum_{ij} (3\gamma_{bi}^{bc}\gamma_{cj}^{bc}-\alpha_{ij}^{bc})I_{bi}I_{cj}$$

$$-C\sum_{ij} (3\gamma_{ci}^{ca}\gamma_{aj}^{ca}-\alpha_{ij}^{ca})I_{ci}I_{aj}$$

$$(3.2)$$

Let

$$D_{ij}^{ab} = -\frac{1}{4}C \left(3\gamma_{ai}^{ab}\gamma_{bj}^{ab} - \alpha_{ij}^{ab}\right)$$
 (3.3)

with similar definitions under cyclic permutations for D_{ij}^{bc} and D_{ij}^{ca} . With these definitions the Hamiltonian, Equation 3.2, may be written

$$H = g\beta(H_{a}I_{a3}^{+H}_{b}I_{b3}^{+H}_{c}I_{c3}^{-1})$$

$$+ 4\sum_{i,j} (D_{ij}^{ab}I_{ai}I_{bj}^{+D_{ij}^{bc}}I_{bi}I_{cj}^{+D_{ij}^{ca}}I_{ci}I_{aj}^{-1})$$
(3.4)

Figure 3.2 shows the matrix representation of Equation 3.4 for the case of protons, $I=\frac{1}{2}$, in the basis indicated and with only the secular terms as described by Andrew⁴ retained. Two eigenvalues may be written down immediately, viz.,

$$E_{1} = \frac{1}{2}g_{\beta}(H_{a} + H_{b} + H_{c}) + D_{33}^{ab} + D_{33}^{bc} + D_{33}^{ca}$$

$$(3.5)$$

$$E_{8} = -\frac{1}{2}g_{\beta}(H_{a} + H_{b} + H_{c}) + D_{33}^{ab} + D_{33}^{bc} + D_{33}^{ca}$$

Table 1. Definitions of direction cosines, $\gamma,$ in the three-dipole triangular configuration

Scalar Product	Direction cosines of:	System
$\vec{I}_a \cdot \vec{p}_{ab} = \sum_i \gamma_{ai}^{ab} I_{ai}$	\vec{p}_{ab}	$(\vec{a}_1, \vec{a}_2, \vec{a}_3)$
1 .		
$\vec{I}_b \cdot \vec{p}_{ab} = \sum_j \gamma_{bj}^{ab} I_{bj}$	\vec{p}_{ab}	$(\vec{b}_1,\vec{b}_2,\vec{b}_3)$
$\vec{I}_b \cdot \vec{p}_{bc} = \sum_i \gamma_{bi}^{bc} I_{bi}$	\vec{p}_{bc}	$(\vec{b}_1, \vec{b}_2, \vec{b}_3)$
ho.	_	
$\vec{I}_{c} \cdot \vec{p}_{bc} = \sum_{j} \gamma_{cj}^{bc} I_{cj}$	\overrightarrow{p}_{bc}	$(\vec{c}_1, \vec{c}_2, \vec{c}_3)$
→	→	<i>→</i> → → ,
$\vec{I}_{c \cdot \vec{p}_{ca}} = \sum_{i} \gamma_{ci}^{ca} I_{ci}$, pca	$(\vec{c}_1, \vec{c}_2, \vec{c}_3)$
†	2	(2 2 2)
$\vec{I}_{c} \cdot \vec{p}_{ca} = \sum_{i} \gamma_{aj}^{ca} I_{aj}$	$\dot{\vec{p}}_{ca}$	$(\vec{a}_1, \vec{a}_2, \vec{a}_3)$

Table 2. Definitions of scalar products, α , between coordinate systems in the three-dipole triangular configuration

Scalar Product		
$\vec{I}_a \cdot \vec{I}_b = \sum_{i,j} \sum_{\alpha ij} \alpha_{ij}^{ab} I_{ai}^{ab}$	$\alpha_{\mathbf{i}\mathbf{j}}^{\mathbf{a}\mathbf{b}} = \overrightarrow{\mathbf{a}}_{\mathbf{i}} \cdot \overrightarrow{\mathbf{b}}_{\mathbf{j}}$	
$\vec{I}_b \cdot \vec{I}_c = \sum_{i j} \alpha_{ij}^{bc} I_{bi}^{cj}$	$\alpha_{\mathbf{i}\mathbf{j}}^{\mathbf{b}\mathbf{c}} = \overrightarrow{\mathbf{b}}_{\mathbf{i}} \cdot \overrightarrow{\mathbf{c}}_{\mathbf{j}}$	
$\vec{I}_{c} \cdot \vec{I}_{a} = \sum_{i j} \alpha_{ij}^{ca} I_{ci}^{l}$	$\alpha_{ij}^{ca} = \vec{c}_{i} \cdot \vec{a}_{j}$	

Figure 3.2 The Hamiltonian matrix for the three photon general case.

	[]	0	0	0	0	0	0	0	[-9/2[HooHboH]] +D22+D22+D23	100 - 00 - 00 100 - 00 - 00
	<u>-</u>	0	0	0	0	(Cf" + C22 +(Cf2 - C2])	[D ₁ , + D ₂ , -iD ₁]}) 22 (일년 [h-h-H]) 2일 - 0일 - 0일 - 0일 - 0일	o	
	[-+-]	0	0	0	0	2년(Ha-Ha-Ha) (Dh. + D호 (다. + D조 -03: -05: -05:31-iDb02:1) -(IDE -02:1)	$\begin{array}{ll} D_{1}^{p_{c}} + D_{2}^{p_{c}} \left\{ \frac{g \beta}{2} \left[H_{0} + H_{0} + H_{1} \right] \left\{ D_{1}^{p_{c}} + D_{2}^{p_{c}} \right\} \\ + \left[D_{1}^{p_{c}} - D_{2}^{p_{c}} \right] - D_{33}^{q_{3}} - D_{33}^{q_{3}} + D_{33}^{q_{3}} \right\} \\ - \left[D_{1}^{p_{c}} - D_{2}^{p_{c}} \right] \end{array}$	- #G	0	
Sis	[+ 2	0	0	0	0	(<u>4</u> /2/44-Hb+Hd {D °+ D22 +D33-D33-D33-i[D2 D21]	(Pr + Dr (4)	{D;; +D;; -[D;; -D;]}	0	FIGURE 3,2
8	[++-]	0		{O!! + D22 +i[D!! -O2!]}	(Dii + D <u>22 {9</u> /2[HaHbaHa] -[[D <u>12 + D21]]-D33+D33 -D33</u> }	O	0	0	0	FIGU
	<u>‡</u>	0	9/3 [H+H+H+H+H] [D]P + D22		(D# + D22 {-	0	0	0	0	
	-÷	0	<u>[Я</u> [Нь+Нь-Нь] :D33-D33-D53	-{[150- 40]:- -{[150- 40]:-	(Df., +D52 +i[Df., -D51]}	0	0	0	0	
	•••	(2011-41-11-11-11-11-11-11-11-11-11-11-11-1	O .	0	0	0	0	0	0	

Upon defining

$$D_{33}^{ab} = -D^{ab}, D_{33}^{bc} = -D^{bc}, D_{33}^{ca} = -D^{ca}$$
 (3.6)

and

$$D_{11}^{ab} + D_{22}^{ab} + i (D_{12}^{ab} - D_{21}^{ab}) = \Delta^{ab}$$

$$D_{11}^{bc} + D_{22}^{bc} + i (D_{12}^{bc} - D_{21}^{bc}) = \Delta^{bc}$$

$$D_{11}^{ca} + D_{22}^{ca} + i (D_{12}^{ca} - D_{21}^{ca}) = \Delta^{ca}$$

$$(3.7)$$

the upper 3 x 3 submatrix becomes

$$\begin{bmatrix}
D_{1} & \Delta^{bc} & \Delta^{ca*} \\
\Delta^{bc*} & D_{2} & \Delta^{ab} \\
\Delta^{ca} & \Delta^{ab*} & D_{3}
\end{bmatrix}$$
(3.8)

where

$$D_{1} = \frac{1}{2}g\beta(H_{a} + H_{b} - H_{c}) + (-D^{ab} + D^{bc} + D^{ca})$$

$$D_{2} = \frac{1}{2}g\beta(H_{a} - H_{b} + H_{c}) + (D^{ab} + D^{bc} - D^{ca})$$

$$D_{3} = \frac{1}{2}g\beta(-H_{a} + H_{b} + H_{c}) + (D^{ab} - D^{bc} + D^{ca})$$
(3.9)

The lower 3 x 3 submatrix becomes

$$\begin{bmatrix}
D_{1}' & \Delta^{bc*} & \Delta^{ca} \\
\Delta^{bc} & D_{2}' & \Delta^{ab*} \\
\Delta^{ca*} & \Delta^{ab} & D_{3}'
\end{bmatrix}$$
(3.10)

where

$$D_{1}' = -\frac{1}{2}g\beta(H_{a}+H_{b}-H_{c}) + (-D^{ab}+D^{bc}+D^{ca})$$

$$D_{2}' = -\frac{1}{2}g\beta(H_{a}-H_{b}+H_{c}) + (D^{ab}+D^{bc}-D^{ca})$$

$$D_{3}' = -\frac{1}{2}g\beta(-H_{a}+H_{b}+H_{c}) + (D^{ab}-D^{bc}+D^{ca})$$
(3.11)

The secular equation for the eigenvalues λ_{i} of Equation 3.8 and Equation 3.10 are obtained in the standard manner, viz., by subtracting λ from the diagonal elements and by equating to zero the determinant of the resulting matrix. Using Equation 3.9 and Equation 3.11, this procedure leads to the very complicated secular equations below, with the upper signs applying to Equation 3.8, and the lower signs to Equation 3.10:

$$\begin{split} & -\lambda^{3} + \lambda^{2} \left[\pm \frac{1}{2} g_{\beta} (H_{a} + H_{b} + H_{c}) + (D^{ab} + D^{bc} + D^{ca}) \right] \\ & + \lambda \left\{ \frac{1}{4} (g_{\beta})^{2} \left[H_{a}^{2} + H_{b}^{2} + H_{c}^{2} - 2(H_{a} H_{b} + H_{b} H_{c} + H_{c} H_{a}) \right] \right\} \\ & \pm g_{\beta} \left[H_{a} (D^{ab} - D^{bc} + D^{ca}) + H_{b} (D^{ab} + D^{bc} - D^{ca}) + H_{c} (-D^{ab} + D^{bc} + D^{ca}) \right] \end{split}$$

$$(3.12)$$

Equation 3.12 continued

$$\begin{split} &+ [(o^{ab})^2 + (o^{bc})^2 + (o^{ca})^2 - 2(o^{ab}o^{bc} + o^{bc}o^{ca} + o^{ca}o^{ab})] \\ &+ [(o^{ab}_{11} + o^{ab}_{22})^2 + (o^{ab}_{12} - o^{ab}_{21})^2 + (o^{bc}_{11} + o^{bc}_{22})^2 + (o^{bc}_{12} - o^{bc}_{21})^2 + (o^{ca}_{11} + o^{ca}_{22})^2 + (o^{ca}_{12} - o^{ca}_{21})^2]) \\ &+ \frac{1}{8} (gg)^3 [H_a^3 + H_b^3 + H_c^3 + 2H_a H_b H_c - H_a^2 (H_b + H_c) - H_b^2 (H_a + H_c) - H_c^2 (H_a + H_b)] \\ &+ \frac{1}{4} (gg)^2 [H_a^2 (o^{ab} - 3o^{bc} + o^{ca}) + H_b^2 (o^{ab} + o^{bc} - 3o^{ca}) + H_c^2 (-3o^{ab} + o^{bc} + o^{ca}) \\ &+ 2H_a H_b (-o^{ab} + o^{bc} + o^{ca}) + 2H_b H_c (o^{ab} - o^{bc} + o^{ca}) + 2H_c H_a (o^{ab} + o^{bc} - o^{ca})] \\ &+ \frac{1}{2} (gg) (H_a [(o^{ab})^2 - 3(o^{bc})^2 + (o^{ca})^2 + 2(o^{ab}o^{bc} + o^{bc}o^{ca} - o^{ca}o^{ab})] \\ &+ H_b [(o^{ab})^2 + (o^{bc})^2 - 3(o^{ca})^2 + 2(o^{ab}o^{bc} + o^{bc}o^{ca} + o^{ca}o^{ab})] \\ &+ H_c [-3(o^{ab})^2 + (o^{bc})^2 - 3(o^{ca})^2 + 2(o^{ab}o^{bc} - o^{bc}o^{ca} + o^{ca}o^{ab})] \\ &- (o^{ab})^3 + (o^{bc})^3 + (o^{ca})^3 + 2o^{ab}o^{bc}o^{ca} - (o^{ab})^2 (o^{bc} + o^{ca}o^{ab})] \\ &+ 2((o^{ab}_{11} + o^{ab}_{22}) (o^{bc}_{11} + o^{bc}_{22}) (o^{ca}_{11} + o^{ca}_{22}) - (o^{ab}_{12} - o^{ab}_{21}) (o^{bc}_{12} - o^{bc}_{21}) (o^{ca}_{11} + o^{ca}_{22}) \\ &- (o^{ab}_{12} - o^{ab}_{21}) (o^{bc}_{11} + o^{bc}_{22}) (o^{ca}_{12} - o^{ca}_{21}) - (o^{ab}_{11} + o^{bc}_{22}) (o^{bc}_{12} - o^{bc}_{21}) (o^{ca}_{12} - o^{ca}_{22}) \\ &+ [(o^{ab}_{11} + o^{ab}_{22})^2 + (o^{ab}_{12} - o^{ab}_{21})^2] [\frac{1}{2} gg(H_a + H_b - H_c) + (o^{ab}_{11} + o^{bc}_{12} - o^{ca}_{11})] \\ &+ [(o^{ab}_{11} + o^{ca}_{22})^2 + (o^{bc}_{12} - o^{bc}_{21})^2] [\frac{1}{2} gg(H_a - H_b + H_c) + (o^{ab}_{11} + o^{bc}_{12} - o^{ca}_{11})] \\ &+ [(o^{ab}_{11} + o^{ca}_{22})^2 + (o^{ab}_{12} - o^{ca}_{21})^2] [\frac{1}{2} gg(H_a - H_b + H_c) + (o^{ab}_{11} + o^{bc}_{12} - o^{ca}_{11})] \\ &+ [(o^{ab}_{11} + o^{ca}_{22})^2 + (o^{bc}_{12} - o^{ca}_{21})^2] [\frac{1}{2} gg(H_a - H_b + H_c) + (o^{ab}_{11} + o^{bc}_{12} - o^{ca}_{11})] \\ &+ [(o^{ab}_{11} + o^{ca}_{12})^2 + (o^{ab}_{12} - o^$$

In order to determine the geometrical dependence of the matrix elements it is necessary to recall the forms of D_{ij}^{ab} , D_{ij}^{bc} , D_{ij}^{ca} , and Δ^{ab} , Δ^{bc} , Δ^{ca} :

$$\begin{split} D_{ij}^{ab} &= -\frac{1}{4} C \left(3 \gamma_{ai}^{ab} \gamma_{bj}^{ab} - \alpha_{ij}^{ab} \right) \\ \Delta^{ab} &= \left(D_{11}^{ab} + D_{22}^{ab} \right) + i \left(D_{12}^{ab} - D_{21}^{ab} \right) \\ &= -\frac{1}{4} C \left[\left(3 \gamma_{a1}^{ab} \gamma_{b1}^{ab} - \alpha_{11}^{ab} \right) + \left(3 \gamma_{a2}^{ab} \gamma_{b2}^{ab} - \alpha_{22}^{ab} \right) \right. \\ &+ i \left(3 \gamma_{a1}^{ab} \gamma_{b2}^{ab} - \alpha_{12}^{ab} \right) - i \left(3 \gamma_{a2}^{ab} \gamma_{b1}^{ab} - \alpha_{21}^{ab} \right) \right] \end{split}$$

The expressions for D_{ij}^{bc} , D_{ij}^{ca} , Δ^{bc} , and Δ^{ca} are found by cyclic permutation of the superscripts.

Careful analysis of Figure 3.3, Figure 3.4, and Figure 3.5 shows that the following geometrical relationships apply:

$$\vec{p}_{ab} \cdot \vec{m}_{ab} = 0 \qquad \vec{p}_{bc} \cdot \vec{m}_{ab} = \cos 30^{\circ} \qquad \vec{p}_{ca} \cdot \vec{m}_{ab} = -\cos 30^{\circ}$$

$$\vec{p}_{ab} \cdot \vec{m}_{bc} = -\cos 30^{\circ} \qquad \vec{p}_{bc} \cdot \vec{m}_{bc} = 0 \qquad \vec{p}_{ca} \cdot \vec{m}_{bc} = \cos 30^{\circ}$$

$$\vec{p}_{ab} \cdot \vec{m}_{ca} = \cos 30^{\circ} \qquad \vec{p}_{bc} \cdot \vec{m}_{ca} = -\cos 30^{\circ} \qquad \vec{p}_{ca} \cdot \vec{m}_{ca} = 0$$

$$\vec{p}_{ab} \cdot \vec{m}_{bc} = \vec{m}_{bc} \cdot \vec{m}_{ca} = \vec{m}_{ca} \cdot \vec{m}_{ab} = -\cos 60^{\circ}$$

$$\vec{p}_{ab} \cdot \vec{p}_{bc} = \vec{p}_{bc} \cdot \vec{p}_{ca} = \vec{p}_{ca} \cdot \vec{p}_{ab} = -\cos 60^{\circ}$$

$$\vec{p}_{ab} \cdot \vec{p}_{bc} = \vec{p}_{bc} \cdot \vec{p}_{ca} = \vec{p}_{ca} \cdot \vec{p}_{ab} = -\cos 60^{\circ}$$

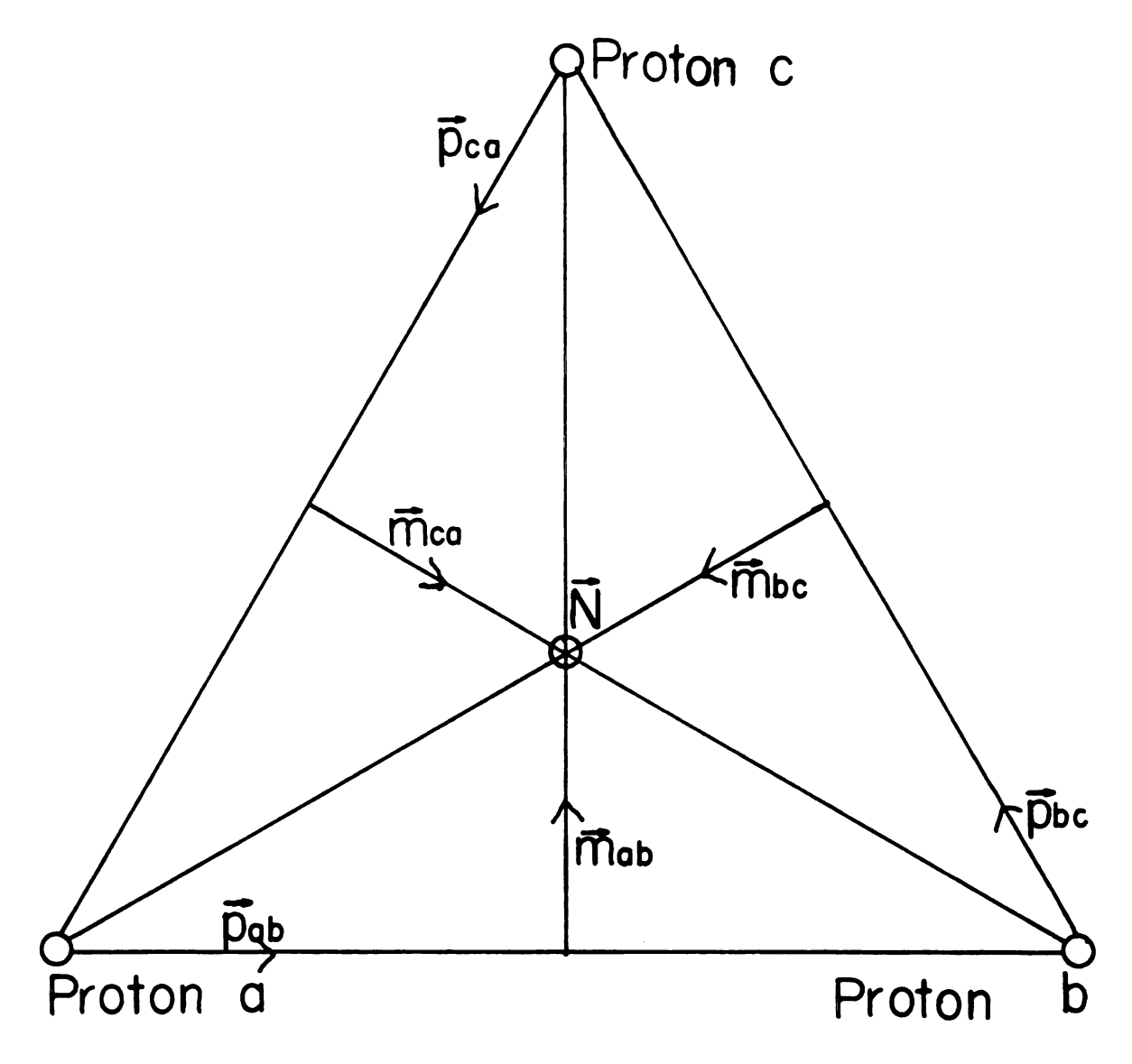


Figure 3.3. Geometric configuration with \vec{N} perpendicular to and directed out of the page. All vectors are coplanar.

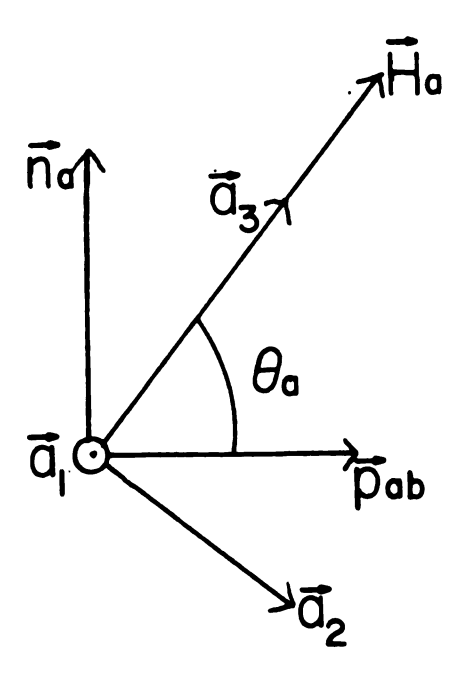


Figure 3.4. Geometric configuration with \vec{a}_1 perpendicular to and directed out of the page. All vectors are coplanar.

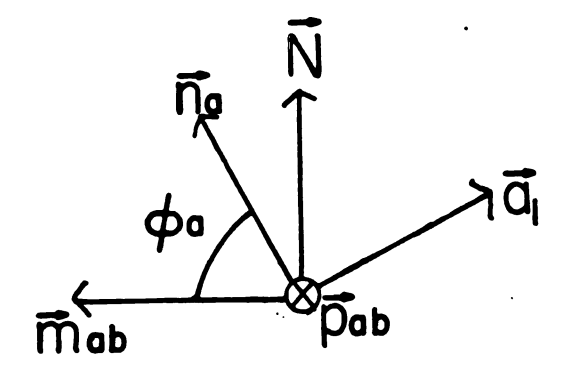


Figure 3.5. Geometric configuration with \vec{p}_{ab} perpendicular to and directed into the page. All vectors are coplanar.

$$\vec{N} \cdot \vec{n}_{a} = \sin \phi_{a} \qquad \vec{n}_{a} \cdot \vec{m}_{ab} = \cos \phi_{a}$$

$$\vec{N} \cdot \vec{n}_{b} = \sin \phi_{b} \qquad \vec{n}_{b} \cdot \vec{m}_{bc} = \cos \phi_{b} \qquad (3.15)$$

$$\vec{N} \cdot \vec{n}_{c} = \sin \phi_{c} \qquad \vec{n}_{c} \cdot \vec{m}_{ca} = \cos \phi_{c}$$

From these relationships, the values of the various $\gamma^{\mbox{ab}}$ and $\alpha^{\mbox{ab}}$ may be developed and one finds:

$$\gamma_{a3}^{ab} = \cos\theta_{a}$$
 $\gamma_{b3}^{ab} = -\cos60^{\circ}\cos\theta_{b} - \cos30^{\circ}\sin\theta_{b}\cos\phi_{b}$

$$\gamma_{a2}^{ab} = \sin\theta_{a}$$
 $\gamma_{b2}^{ab} = -\cos60^{\circ}\sin\theta_{b} + \cos30^{\circ}\cos\theta_{b}\cos\phi_{b}$

$$\gamma_{a1}^{ab} = 0$$
 $\gamma_{b1}^{ab} = \cos30^{\circ}\sin\phi_{b}$

 $\alpha_{33}^{ab} = \sin\theta_a \sin\theta_b \sin\phi_a \sin\phi_b - \cos60^{\circ} \sin\theta_a \sin\theta_b \cos\phi_a \cos\phi_b$

 $-\cos 60^{\circ} \cos \theta_{a} \cos \theta_{b} + \cos 30^{\circ} \sin \theta_{a} \cos \theta_{b} \cos \phi_{a}$

 $-\cos 30^{\circ} \sin \theta_b \cos \theta_a \cos \phi_b$

$$\alpha_{22}^{ab} = \cos\theta_a \cos\theta_b \sin\phi_a \sin\phi_b - \cos60^\circ \cos\theta_a \cos\phi_b \cos\phi_b \cos\phi_b$$
 (3.16)

 $-\cos 60^{\circ} \sin \theta_a \sin \theta_b + \cos 30^{\circ} \sin \theta_a \cos \theta_b \cos \phi_b - \cos 30^{\circ} \cos \theta_a \sin \theta_b \cos \phi_a$

$$\alpha_{11}^{ab} = -\cos 60^{\circ} \sin \phi_a \sin \phi_b + \cos \phi_a \cos \phi_b$$

 $\alpha_{12}^{ab} = -\cos 30^{\circ} \sin \theta_b \sin \phi_a - \cos 60^{\circ} \cos \theta_b \sin \phi_a \cos \phi_b - \cos \theta_b \cos \phi_a \sin \phi_b$

 $\alpha_{21}^{ab} = \cos 30^{\circ} \sin \theta_a \sin \phi_b - \cos 60^{\circ} \cos \theta_a \cos \phi_a \sin \phi_b - \cos \theta_a \sin \phi_a \cos \phi_b$

Cyclic permutation gives the corresponding expressions for γ^{bc} , α^{bc} , γ^{ca} , and α^{ca} .

Consider now the special case of equal fields for which $\vec{a}_3 = \vec{b}_3 = \vec{c}_3$. When \vec{a}_3 and \vec{b}_3 are written out in terms of their components in the \vec{N} , \vec{m}_{ab} , and \vec{p}_{ab} directions, the following relations apply:

(a)
$$\vec{b}_3 \cdot \vec{p}_{bc} = \vec{a}_3 \cdot \vec{p}_{bc}$$

(b) $\vec{b}_3 \cdot \vec{N} = \vec{a}_3 \cdot \vec{N}$ (3.17)
(c) $\vec{b}_3 \cdot \vec{m}_{bc} = \vec{a}_3 \cdot \vec{m}_{bc}$

or more explicitly:

(a)
$$\cos\theta_b = -\cos 60^{\circ} \cos\theta_a + \cos 30^{\circ} \sin\theta_a \cos\phi_a$$

(b) $\sin\theta_b \sin\phi_b = \sin\theta_a \sin\phi_a$
(c) $\sin\theta_b \cos\phi_b = -\cos 60^{\circ} \sin\theta_a \cos\phi_a - \cos 30^{\circ} \cos\theta_a$
(3.18)

These equations specify the relationship between (θ_a, ϕ_a) and (θ_b, ϕ_b) when $\vec{H}_a = \vec{H}_b$, and examination of these equations shows that indeed a particular choice of (θ_a, ϕ_a) uniquely determines (θ_b, ϕ_b) , and vice versa. Cyclic permutation of indices yields the sets of equations which relate (θ_b, ϕ_b) to (θ_c, ϕ_c) , and (θ_c, ϕ_c) to (θ_a, ϕ_a) , respectively.

Substitution of Equations 3.18 into the expressions for $\alpha_{33}^{ab} = \vec{a}_3 \cdot \vec{b}_3$ yields unity, as required for equal fields. Furthermore, with

$$\gamma_{a3}^{ab} = \gamma_{b3}^{ab} = \cos\theta_a$$
, cyclic (3.19)

the diagonal elements D^{ab} etc., are found to reduce to $\frac{1}{4}$ C ($\cos^2\theta_a$ -1), cyclic, which agrees with the corresponding results of Andrew and Bersohn.

Despite much effort, no analytical method was found that would show that the off-diagonal matrix elements Δ^{ab} , Δ^{bc} , and Δ^{ca} reduce to those of Andrew and Bersohn when Equations 3.18 hold. Instead, a particular numerical choice for θ_a and ϕ_a was made (viz., θ_a =43° ϕ_a =27°), and for that choice, and with Equations 3.18 applying, it was found that the resulting cubic secular equations agreed with those obtained from Andrew and Bersohn's paper.

It seems obvious that an exact analytic solution for Equation 3.12 cannot easily be found. Perturbation theory is not particularly helpful either, since for a degenerate or nearly degenerate zero-order subblock, perturbation theory calls for diagonalizing that block, i.e., the exact solution of Equation 3.12.

There is, however, a physically interesting special case for which computing numerical solutions becomes practicable. This case will be treated in the next chapter.

CHAPTER IV

THE SYMMETRICAL CANTING CASE

The symmetrical canting case is defined as the case for which

$$\theta_{a} = \theta_{b} = \theta_{c} = \theta$$

$$\phi_{a} = \phi_{b} = \phi_{c} = \phi$$

$$H_{a} = H_{b} = H_{c} = H$$

$$(4.1)$$

In this case,

$$\gamma_{a3}^{ab} = -\gamma_{b3}^{ab} \tag{4.2}$$

as seen in Figure 4.1. As a consequence, Equations 3.16 give

$$\cot\theta = 2\cos 30^{\circ}\cos\phi$$
 (4.3)

This equation determines the angle ϕ for a given θ , and vice versa. The following three special cases of Equation 4.3 may be considered:

a)
$$\theta = 30^{\circ}$$
, $\phi = 0^{\circ}$
b) $\theta = 90^{\circ}$, $\phi = 90^{\circ}$ (4.4)
c) $\theta = 150^{\circ}$, $\phi = 180^{\circ}$

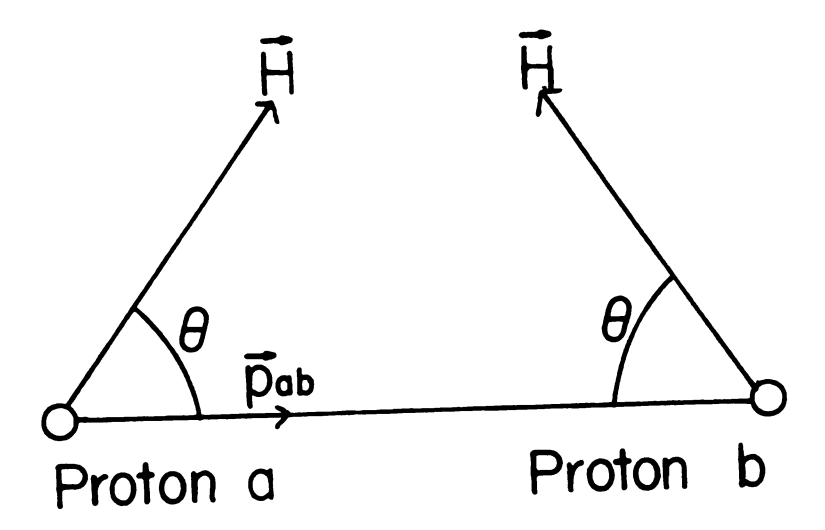


Figure 4.1. The symmetrical canting case as seen in the plane containing \hat{p}_{ab} and \hat{H} at the proton a site.

where a) is the case in which H is in the plane of the proton triangle and directed radially inward; b) is the case in which H is perpendicular to the plane of the triangle; and c) is the case in which H is in the plane of the triangle and directed radially outward.

The relevant scalar products become, upon inserting Equation 4.1 and Equation 4.2 into Equation 3.16,

$$\begin{array}{lll} \gamma_{a1}^{ab} = 0 & \gamma_{b1}^{ab} = \cos 30^{\circ} \sin \varphi \\ \\ \gamma_{a2}^{ab} = \sin \theta & \gamma_{b2}^{ab} = -\cos 60^{\circ} \sin \theta + \cos 30^{\circ} \cos \theta \cos \varphi \\ \\ \gamma_{a3}^{ab} = \cos \theta & \gamma_{b3}^{ab} = -\cos \theta \\ \\ \alpha_{33}^{ab} = 1 - 2 \cos^2 \theta & \\ \\ \alpha_{22}^{ab} = \cos^2 \theta \sin^2 \phi - \frac{1}{2} \cos^2 \theta \cos^2 \phi - \frac{1}{2} \sin^2 \theta \\ \\ \alpha_{11}^{ab} = -\frac{1}{2} \sin^2 \phi + \cos^2 \phi \\ \\ (\alpha_{21}^{ab} - \alpha_{21}^{ab}) = \sqrt{3} \sin \theta \sin \phi \end{array} \tag{4.5}$$

With Equation 4.3, the following relationship is seen to hold:

$$(\gamma_{b1}^{ab})^2 + (\gamma_{b2}^{ab})^2 + (\gamma_{b3}^{ab})^2 = 1$$
 (4.6)

The relationships for D^{ab} and Δ^{ab} follow from Equation 4.5, viz.,

$$D = D^{ab} = D^{bc} = D^{ca} = -\frac{1}{4} C (1 + \cos^2 \theta)$$

$$\Delta = \Delta^{ab} = \Delta^{bc} = \Delta^{ca} = \frac{1}{8} C (1 - 3\cos^2 \theta + 3\sin^2 \theta \cos^2 \phi)$$

$$+ (i/8) C (\sqrt{3} \sin \theta \sin \phi)$$
(4.7)

The following eigenvalues may be written down immediately:

$$E_1 = \frac{3}{2}g\beta H + 3D$$

$$(4.8)$$

$$E_8 = -\frac{3}{2}g\beta H + 3D$$

The remaining six eigenvalues are

$$E_{i} = \frac{1}{2}g\beta H + \lambda_{i}$$
 (i=1,2,3)
 $E_{j} = -\frac{1}{2}g\beta H + \lambda_{j}$ (j=1,2,3)

where the $\lambda_{\hat{1}}$ are the three eigenvalues of the upper 3 x 3 Hamiltonian submatrix with associated secular equation

In more explicit form,

$$\lambda^{3} - 3D\lambda^{2} + 3(D^{2} - |\Delta|^{2})\lambda - D^{3} + 3D|\Delta|^{2} - 2\Delta_{r}^{3} + 6\Delta_{r}\Delta_{i}^{2} = 0$$
(4.11)

where $\Delta_{\mathbf{r}}$ is the real part of Δ and $\Delta_{\mathbf{i}}$ is the imaginary part. The associated eigenvalues were determined numerically as a function of θ . They are listed in Table 3 and plotted in Figure 4.2. The lower 3 x 3 submatrix is found to have eigenvalues given by Equation 4.9, with the $\lambda_{\mathbf{j}}$ identical with the $\lambda_{\mathbf{j}}$ of Equation 4.10.

In the special case when $\theta \! = \! \varphi \! = \! 90^{\circ}$, it can be seen from Figure 4.3 that

$$\gamma_{a1}^{ab} = 0 \qquad \gamma_{b1}^{ab} = \frac{1}{2}\sqrt{3} \qquad \alpha_{11} = -\frac{1}{2} \qquad \alpha_{12} = -\frac{1}{2}\sqrt{3} \\
\gamma_{a2}^{ab} = 1 \qquad \gamma_{b2}^{ab} = -\frac{1}{2} \qquad \alpha_{22} = -\frac{1}{2} \qquad \alpha_{21} = \frac{1}{2}\sqrt{3} \qquad (4.12) \\
\gamma_{a3}^{ab} = 0 \qquad \gamma_{b3}^{ab} = 0 \qquad \alpha_{33}^{ab} = 1$$

The general expressions, Equation 3.16, and the symmetrical canting expressions, Equation 4.5, are found to reduce properly to the above values. Furthermore one has that here

$$D = -\frac{1}{4}C$$

$$\Delta = -\frac{1}{4}C e^{-i(2\pi/3)}$$
(4.13)

which checks Andrew and Bersohn's results except for the constant phase factor. It has been verified that the same secular equation is obtained with or without the phase factor, which is connected with the rotation \vec{b}_1 , \vec{b}_2 , \vec{b}_3 relative to \vec{a}_1 , \vec{a}_2 , \vec{a}_3 by $2\pi/3$ for this special case.

Table 3. The eigenvalues of the upper 3 x 3 submatrix as a function of θ in units of $C=(g\beta)^2R^{-3}$.

θ	ф	λ ₁	λ ₂	λ ₃
(degrees)	(degrees)	c		c
30	0	37500	37500	56250
35	34.45795	25334	49737	50254
40	46.52332	20008	54992	44031
45	54.73561	15853	59147	37500
50	61.02327	12371	62629	30987
60	70.52878	06878	68120	18752
70	77.86954	03039	71954	08780
80	84.15703	00745	74239	02278
90	90.00000	.00000	75000	.00000
100	95.84297	00745	74239	02278
110	102.13046	03039	71954	08780
120	109.47122	06878	68120	18752
130	118.97673	12371	62629	30987
135	125.26439	15853	59147	37500
140	133.47668	20008	54992	44031
145	145.54205	25334	49737	50254
150	180.00000	37500	37500	56250

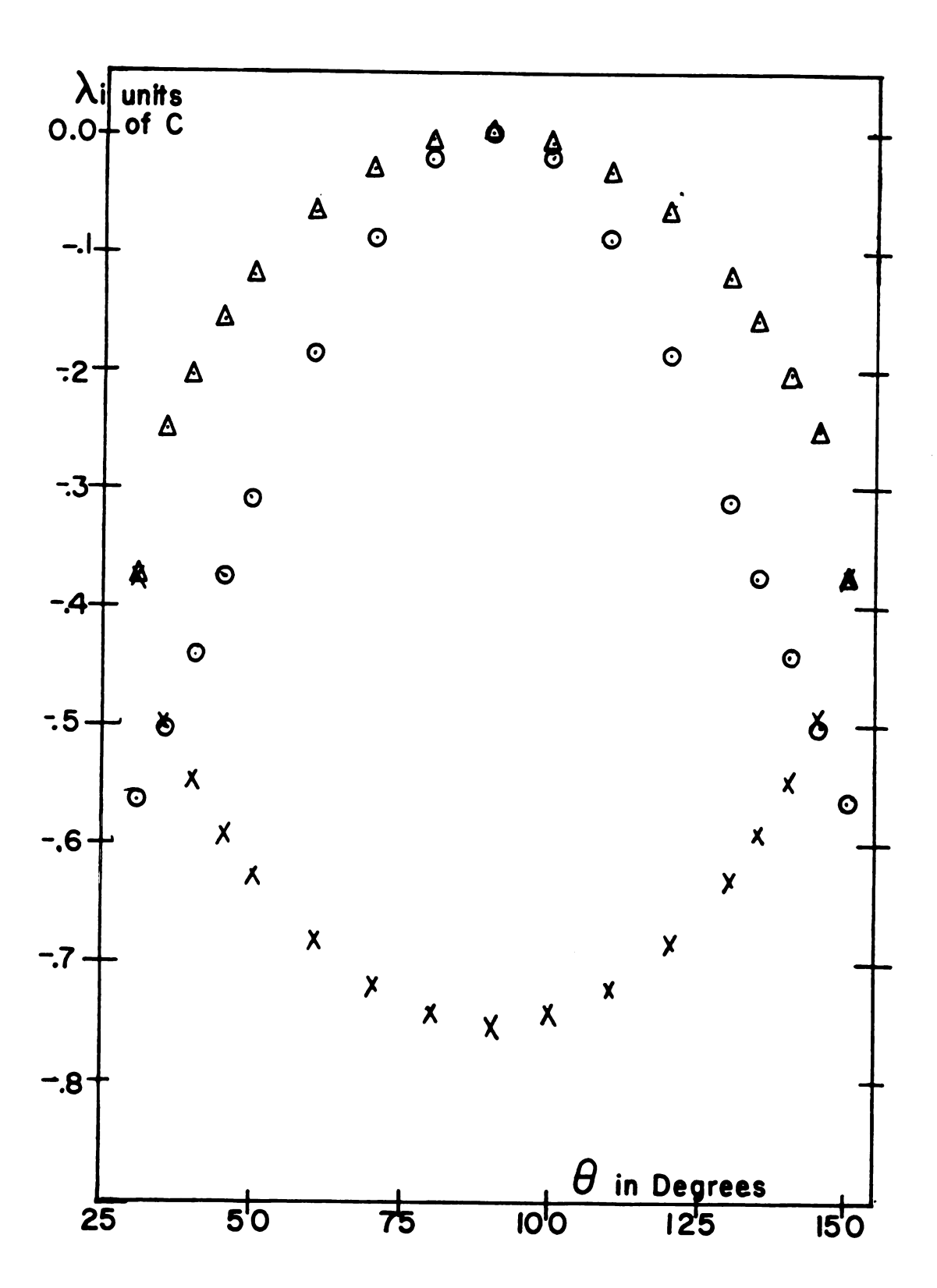
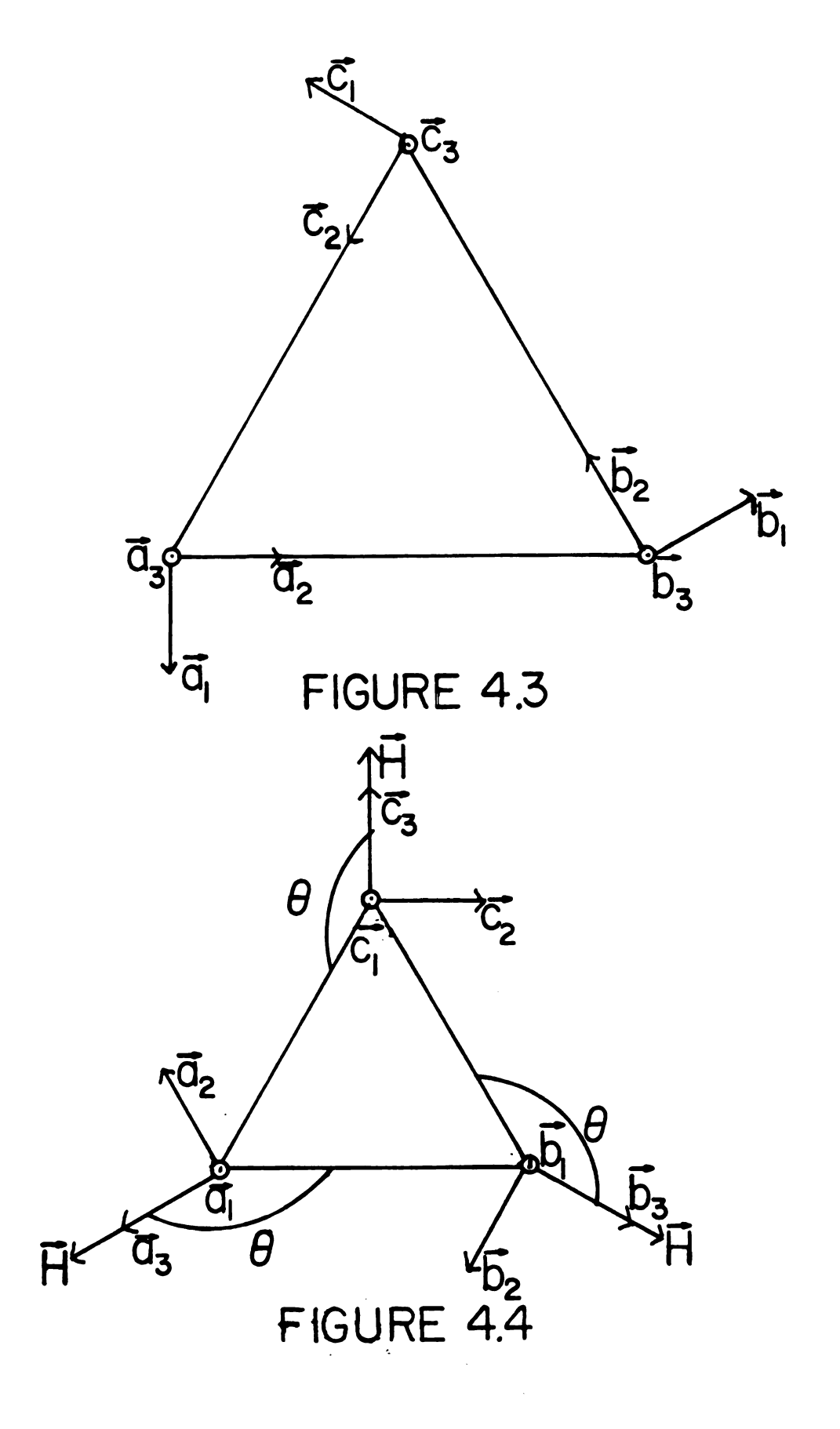


Figure 4.2. The eigenvalues of the symmetrical canting case as a function of $\boldsymbol{\theta}.$

Figure 4.3. The geometric configuration for $\theta=\varphi=90^\circ.$ In this case $\vec{a}_3=\vec{b}_3=\vec{c}_3$ and directed out of the page.

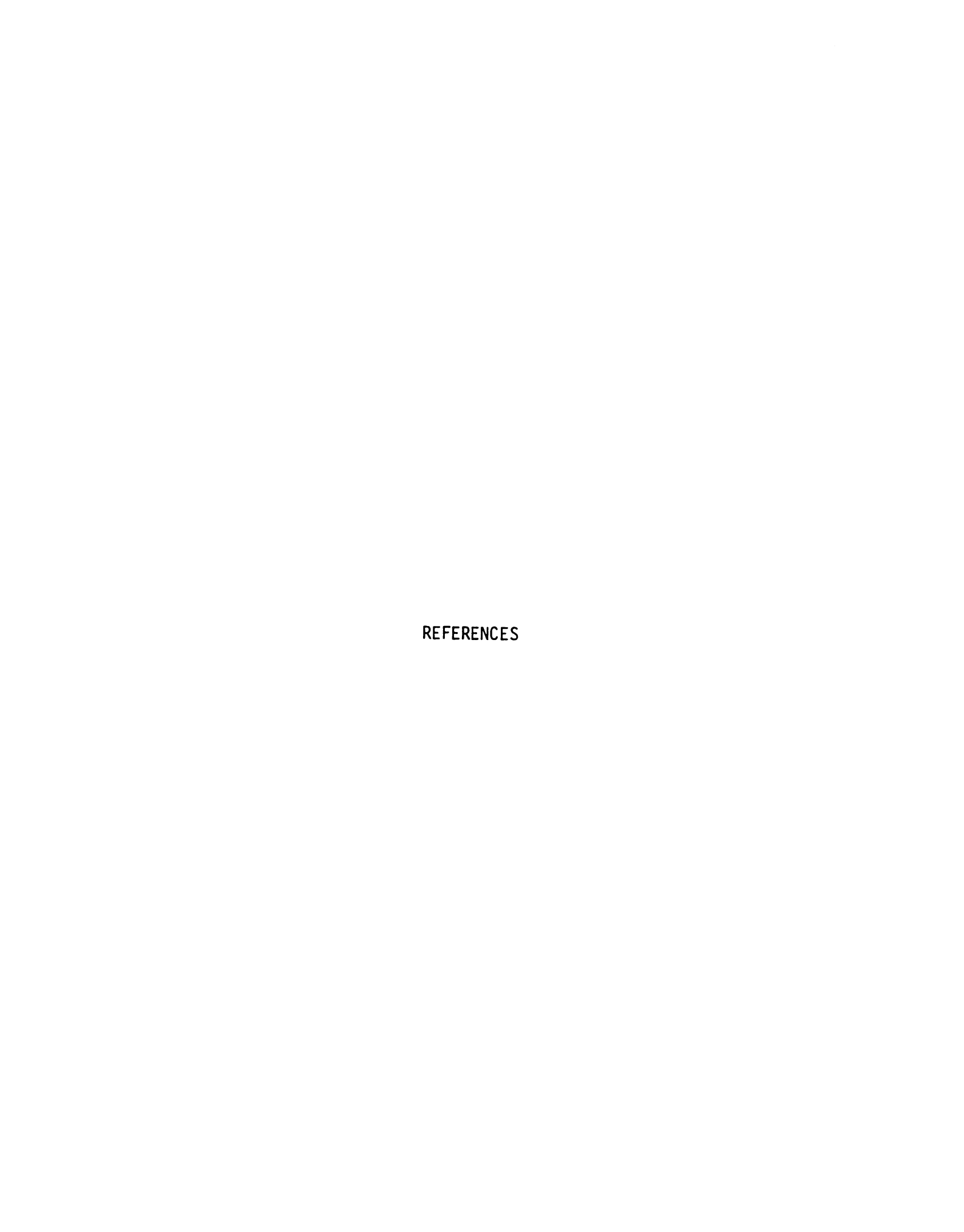
Figure 4.4. The geometric configuration for θ =150°, ϕ =180°. In this case \vec{a}_1 = \vec{b}_1 = \vec{c}_1 and directed out of the page.



In the special case where $\theta\text{=}150^{\circ}$ and $\varphi\text{=}180^{\circ}\text{, as in Figure 4.4,}$

$$\gamma_{a1}^{ab} = 0 \qquad \gamma_{b1}^{ab} = 0 \qquad \alpha_{33}^{ab} = -\frac{1}{2} \qquad \alpha_{12}^{ab} = 0 \\
\gamma_{a2}^{ab} = \frac{1}{2} \qquad \gamma_{b2}^{ab} = \frac{1}{2} \qquad \alpha_{11}^{ab} = 1 \qquad \alpha_{21}^{ab} = 0 \\
\gamma_{a3}^{ab} = -\sqrt{3}/2 \qquad \gamma_{b3}^{ab} = \sqrt{3}/2 \qquad \alpha_{22}^{ab} = -\frac{1}{2}$$
(4.14)

again determined by inspection. The symmetrical canting expressions, Equation 4.5, once more reduce properly to the above values.



REFERENCES

- 1. R. D. Spence and A. C. Botterman, Phys. Rev. B 9, 2993 (1974).
- 2. G. E. Pake, J. Chem. Phys. 16, 327 (1948).
- 3. E. R. Andrew and R. Bersohn, J. Chem. Phys. <u>18</u>, 159 (1950).
- 4. E. R. Andrew, <u>Nuclear Magnetic Resonance</u>, (Cambridge at the University Press, London, 1955).
- 5. G.E.G. Hardeman, <u>Resonantie en Relaxatie Van Protonspins in een Antiferromagnetisch Kristal</u>, (Riksuniveisiteit Te Leiden, 1954).

